Venous Catheter Based Mapping of Ectopic Epicardial Activation: Training Data Set Selection for Statistical Estimation

Bülent Yılmaz*, Robert S. MacLeod, *Member, IEEE*, Bonnie Billard Punske, Bruno Taccardi, and Dana H. Brooks, *Member, IEEE*

***Abstract*—A source of error in most of the existing catheter cardiac mapping approaches is that they are not capable of acquiring epicardial potentials even though arrhythmic substrates involving epicardial and subepicardial layers account for about 15% of the ventricular tachycardias. In this subgroup of patients, mapping techniques that are limited to the endocardium result in localization errors and failure in subsequent ablation procedures. In addition, catheter-based electrophysiological studies of the epicardium are limited to regions near the coronary vessels or require transthoracic access. We have developed a statistical approach by which to estimate high-resolution maps of epicardial activation from very low-resolution multi-electrode venous catheter measurements. A training set of previously recorded maps is necessary for this technique so that composition of the database becomes an important determinant of accuracy. The specific hypothesis of the study was that estimation accuracy would be best when the training data set matches that of the test beat(s), whereby the matching was according to the site of initiation of the beats. This hypothesis suggests approaches to optimized selection of the training set, three of which we have developed and evaluated. One of these methods, the high-CC refinement method, was able to estimate the earliest activation site of left ventricularly paced maps within an average of 4.67 mm of the true site; in 89% of the cases (a total of 231 cases) the error was smaller than 10 mm. In another method, MHC-Spatial activation, right ventricularly paced maps (239 maps) were estimated with an error of 7.15 mm. The average correlation coefficient between the original and the estimated maps was also very high (0.97), which shows the ability of the training data set refinement methods to estimate the epicardial activation sequence. The results of these tests support the hypothesis and, moreover, suggest that such an approach is feasible for providing accurate reconstruction of complete epicardial activation-time maps in a clinical setting.**

***Index Terms*—Catheter mapping, epicardial activation mapping, statistical estimation, training set selection.**

Manuscript received July 3, 2004; revised February 20, 2005. This work was supported by the Whitaker Foundation, the Nora Eccles Treadwell Foundation, the Richard A. and Nora Eccles Harrison Fund for Cardiovascular Research, and the National Institutes of Health (NIH) National Center for Research Resources (NCRR). *Asterisk indicates corresponding author.*

*B. Yılmaz, is with the Biomedical Engineering Department of Başkent University, 06530 Ankara, Turkey (e-mail: byilmaz@baskent.edu.tr(e-mail: byilmaz@baskent.edu.tr).

R. S. MacLeod, B. B. Punske, and B. Taccardi are with The Nora Eccles Harrison Cardiovascular Research and Training Institute, University of Utah, Salt Lake City, UT 84112-5000 USA (e-mail: macleod@cvrti.utah.edu; punske@cvrti.utah.edu; taccardi@cvrti.utah.edu).

D. H. Brooks is with the Center for Communications and Digital Signal Processing (CDSP), Northeastern University, Boston, MA 02115-5000 USA (e-mail: brooks@ece.neu.edu).

Digital Object Identifier 10.1109/TBME.2005.856243

I. Introduction

In this paper, we describe progress in an approach for cardiac mapping based on predicting high-resolution epicardial activation maps from sparse multi-electrode venous catheter measurements using a statistical estimation technique. Cardiac mapping is a method that involves the acquisition and display of spatial distributions of cardiac electric potential as functions of time (isopotential mapping) or of the time of activation (isochrone mapping) [25]. One of the main objectives of cardiac mapping is to detect and analyze the path of reentry, especially the activation wavefronts emerging from regions of abnormally slow conduction that are known to play a key role in arrhythmogenesis [18]. Correct localization of such substrates is critical for understanding the pathophysiologic mechanisms of cardiac rhythm disturbances, evaluating the effect of a drug, or directing surgical and catheter ablation techniques.

Catheter-based approaches to cardiac mapping have revolutionized the field of arrhythmia diagnosis and treatment because they do not require thoracotomy. The systems that have been developed over the last 20 years for this purpose include commercial systems that enable mapping by means of localizable catheters [15] and [42], noncontact multi-electrode catheters [2], [5], [33], balloon and superelastic, collapsible, basket-shaped contact catheters [11], [13], [32], magnetically guided catheters [14], and bi-plane navigational catheters [12].

A source of error in most of the existing approaches is that they are not capable of acquiring data from the epicardium even though arrhythmic substrates involving epicardial and subepicardial layers account for about 15% of the ventricular tachycardias [20], [24]. In this subgroup of patients, mapping techniques that are limited to the endocardium result in localization errors and failure in subsequent ablation procedures. Several authors [4], [7], [34], [39] have recently reported unsuccessful endocardial ablation procedures due to epicardial origin of the reentrant pathways, which required subsequent epicardial mapping either by open-chest surgery or by transthoracic mapping and ablation. In 1996, Sosa *et al.* [38] developed a technique to introduce a standard ablation catheter into the pericardial space through a puncture in the subxiphoid region [36], [37]. Although this technique provides access to the epicardium, its elevated level of invasiveness makes its use difficult to justify if there is not strong evidence of epicardial involvement. Thus, there is a well-defined need to develop less invasive techniques that are capable of measuring and/or computing excitation times not only from the endocardium but also over the epicardium. Therefore, we

concentrated in this study on epicardial mapping even though the approaches we describe also apply to endocardial mapping.

The aim of these studies is to use multi-electrode coronary venous catheters to carry out mapping of the epicardium. Such techniques are widely used to diagnose and treat supraventricular arrhythmias, however, their application to the epicardium is severely limited because of much of the heart does not lie close to a major vessel segment.

We have shown that even elaborate interpolation schemes are inadequate for the sparse electrode arrangements in this problem, especially in their ability to identify accurately focal sites of early activation [22]. In the same study we described a statistical estimation technique by which it is possible to reconstruct the activation pattern over the entire epicardium using only values measured from venous catheter electrode recordings. This technique uses a linear estimation model that derives a relationship between venous catheter measurements and unmeasured epicardial sites from a set of previously recorded, high-resolution epicardial activation maps used as a training data set.

The main purpose of this study was to address systematically and comprehensively the relationship between training data set selection and estimation accuracy and thus bring the technique closer to clinical utility. This topic has challenged investigators for many years in a large number of application areas, for example, pattern recognition [17], [19], [31], pattern classification [3], medical image segmentation [6], and remote sensing [40]. The specific hypothesis of the present study was that training data sets matched in some way to the test activation map would perform better than training sets containing a broader, more diverse, mix of activation maps, where the matching criterion was based on the earliest activation site of the beats. If correct, this hypothesis suggests approaches to optimizing selection of the training data set, three of which we have developed and evaluated.

Our evaluation of this hypothesis and the resulting estimation methods was based on a database of 470 beats recorded from 12 different animals. We sampled the epicardial potentials using a flexible sock electrode array containing 490 unipolar electrodes and stimulated the activations via unipolar pacing from all over the epicardium. The study involved selecting subsets of the full database that, to varying degrees, matched the test beats on the basis of site of earliest activation. We first selected the training set manually with full knowledge of the test beat activation maps and found that estimation accuracy improved as the earliest activation site of the training beats more closely matched that of the test beat. We then applied several algorithms to automatically select the composition of the training set without explicit knowledge of the test beat map, but rather based only on the knowledge of the test beat activation times at the surrogate catheter lead sites. The results of these tests supported our hypothesis and, moreover, suggest that such an approach is feasible for providing accurate reconstruction of complete venous catheter-based epicardial activation-time maps in a clinical setting.

II. Methods

A. Experimental Setup and Data Acquisition

In all the experiments from this study we used a 490-electrode sock array to record epicardial electrograms from dog hearts.

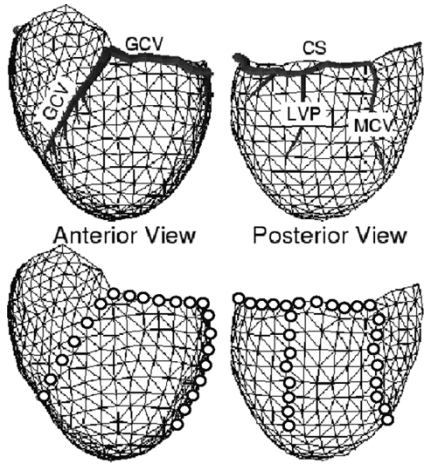

Fig. 1. Diagram representing the 490-lead epicardial electrode sock. Each node of the mesh represents a single silver-wire electrode; the 42 leads used as a surrogate catheter subset are indicated by larger dots. The top row contains the anterior and posterior view of the sock including coronary vessels and the lower row show the sets of nodes on the sock corresponding to the 42-lead subset. The vessels include the great cardiac vein (GCV), the coronary sinus (CS), the left ventricular posterior vein (LVP), and the middle cardiac vein (MCV).

The layout of the electrodes followed markings on a mold of a medium sized dog heart, with a mean interelectrode distance of 4.3 mm. The same heart mold also contained the locations of the coronary vessels, from which we defined a 42-lead surrogate catheter subset to lie along the major veins, as shown in Fig. 1. Our previous studies have shown the equivalence of electrograms recorded from venous catheter and epicardial contact electrodes [22], which provides a simple means of both gathering the required test data and evaluating the results. Markings on the sock of anatomic landmarks, such as left anterior descending artery (LAD), provided consistent—although clearly not identical—placement of the electrodes across experiments.

We performed 12 separate experiments using two different types of animal preparations, both of which were approved by our institution's animal care and use committee, to create the epicardial activation map database. The first preparation used an *in situ* canine heart model in which anesthetized dogs were midsternally incised and the exposed hearts suspended in a pericardial cradle. The second preparation used isolated dog hearts suspended in a torso-shaped, isotonic electrolyte-filled tank. A support dog provided the blood for the isolated heart. From the resulting 823 recorded heart beats, we created a database for this study that included 470 maps, each paced from a unique site (239 from the right ventricle and 231 from the left ventricle). The purpose of using single site stimulation was to simulate the early activation that occurs from both the exit sites in reentry and the focal activation that occurs in ectopic tachycardias. 96% of the maps came from the *in situ* preparation and 90% came from healthy hearts. In the remaining experiments we applied interventions that included localized heating and cooling, local injection of procainamide (a Class I antiarrhythmic drug), infusion of ethanol into a coronary artery, a five day old infarction, and acute restriction of coronary artery flow.

The custom-built measurement system used for the study saved signals continuously to magnetic disk from up to 1024 simultaneous channels with 1 kHz sampling rate and 12-bit resolution. Processing of the resulting recordings consisted

of selecting one representative beat from each three-second recording. Determination of activation times was by means of the minimum slope during the QRS complex of each of the electrograms. When the signal quality was low due to poor contact or broken leads (which occurred in less than 4% of all measurements), we applied wave-equation-based interpolation [28] to compute the potential values at the locations for which measured signals were not available. We then manually checked each resulting activation map for anomalous features or obvious errors using our custom-built visualization software [26].

B. Linear Estimation Method

Details of the estimation algorithm have been reported elsewhere [23]. Briefly, we first defined a training database consisting of up to 470 activation-time maps and selected the surrogate catheter leadset (42 leads) as a subset of the 490-lead sock. We assumed that those 42 leads contained "known" values (surrogates for the venous catheter leads) and the remaining 448 leads (for which we wished to estimate values) contained "unknown" activation values. We reordered the training set in such a way that the activation times for a given beat were treated as elements of a column vector, and then the various beats stacked side-by-side to form a matrix, $\mathbf{A}$, such that the known values comprised the first 42 rows of the matrix. We then calculated the covariance matrix, $\mathbf{C}$, by the usual means. We then formed a transformation matrix, $\mathbf{T}$, to be used to estimate the activation-times at the unmeasured sites as

$$\mathbf{T} = (\mathbf{C_{uk}})^{\mathbf{T}}(\mathbf{C_{kk}})^{-\mathbf{1}} \tag{1}$$

where $\mathbf{C_{kk}}$ and $\mathbf{C_{uk}}$ are submatrices of $\mathbf{C}$ representing the auto-covariance of the known leads and the cross-covariance of known and unknown leads, respectively. $\mathbf{T}$ is a matrix of basis vectors unique to the training set such that left multiplication by $\mathbf{T}$ of any measurement vector of the 42 leads (with some manipulation to take care of the means, see (2)) yields an estimate of the activation values at all remaining sites and thus a complete, high-resolution map

$$A_U^i = \mathbf{T} \times \left(A_K^i - \overline{A}_K\right) + \overline{A}_U \tag{2}$$

where A_K^i and A_U^i are the measured and estimated portions, respectively, of the i'th map. $\overline{A}_K$ and $\overline{A}_U$ are the rows of the first column of $\overline{\mathbf{A}}$ that correspond to the known and unknown leads, respectively. In the computation of the inverse of $\mathbf{C_{kk}}$, we used the truncated singular-value decomposition technique [30] when the condition number (ratio between the largest and smallest singular value) of the $\mathbf{C_{kk}}$ matrix was greater than 100 000. The number of singular values used in the truncation was set equal to the number of largest singular values whose summation comprised 99% of the cumulative sum of all of them.

C. Testing Paradigms and Error Metrics

To evaluate the performance of the estimation, we used a "leave-one-out" protocol (LMap), in which we kept the map to be estimated (test map) out of the data set and trained the transformation matrix with the remaining maps. Repeating this process for each of the maps in the database and then comparing each test map to the associated estimate provided a means of computing overall statistics that included beats from a range of pacing sites.

We used two different metrics: the Euclidean distance between the actual and the estimated site of earliest activation, LDist, and the absolute difference in activation times between the actual and the estimated site of earliest activation, $\Delta\mathrm{T_{EA}}$. LDist and $\Delta\mathrm{T_{EA}}$ are thereby specific and clinically relevant measures based on the anticipated use of such a procedure. A further metric of overall performance was the percentages of cases in which the error fell into one of three ranges: 1) $\mathrm{LDist} < \mathrm{MinRes}$, in which LDist was smaller than it was possible to resolve between electrodes, 2) $\mathrm{LDist} < 5$ mm, in which LDist was smaller than 5 mm, and 3) $\mathrm{LDist} < 10$ mm, in which LDist was smaller than 10 mm. Histograms of the error metrics indicated a non-Gaussian distribution and thus we applied a Wilcoxon rank-sum test for pairwise comparisons and a Kruskal-Wallis test for comparisons among more than two samples to determine statistical significance between different optimization strategies $(p = 0.05)$.

D. Effect of Training Set Selection

In a preliminary study [43], we found that selection of the training data set affected the accuracy of the resulting estimation, so here we set out to examine this behavior in more detail. We sought to determine specifically what constitutes a good training set, how to select one *a priori*, and whether a refinement scheme can improve on a first-guess training set.

In order to address the first question, we tested two different approaches for selecting a good training set. We either maximized the variety of maps in the training set, i.e., ensuring that the training set included maps paced from wide range of sites or maximized the similarity of the maps in the training set to the map to be reconstructed (test map) according to some matching feature.

Here we evaluated training sets that included beats paced from the first, second, and third order neighbors around the pacing site of the test beat. We compared the results of these matched training sets to the entire database ("all maps estimate" or AME). Matched training sets included the maps from the database that were paced from the first order ("F"), first and second order ("F + S"), or first, second, and third order ("F + S + T") neighboring electrodes as shown in Fig. 2. Evaluation of each estimate was by means of visual examination and the LDist and $\Delta\mathrm{T_{EA}}$ error metrics.

E. Uninformed Selection of Training Sets

An important component of this study was to evaluate several training data set selection schemes that do not require any *a priori* information about the site of earliest activation.

Our approach was to find a good first guess (estimate) based on either all maps in the database or a substantial subset and then refine the training set—select matched training sets automatically—using different strategies. The first guess was based either on the entire database, the AME first guess, or from a subset of training maps that were well correlated with the test beat based on the 42-lead subset common to both, referred to as the "most highly correlated" (MHC) first guess. The idea behind the correlation-based first guess method was that the maps in the database that were similar to the test map should have similar waveforms in the corresponding 42 measured leads so we could select the beats that were highly correlated. We then

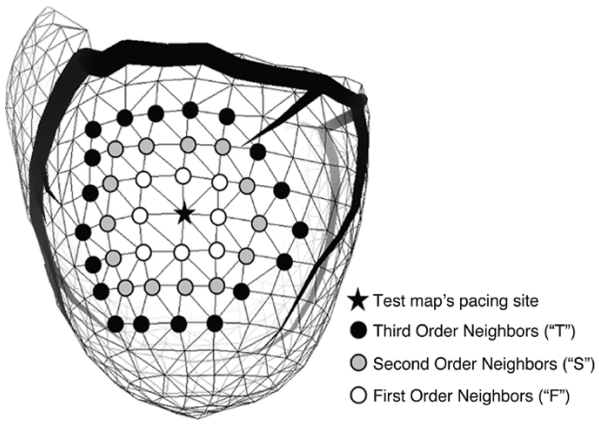

Fig. 2. Description of different orders of neighbors. Labeled with shaded ellipses are the first, second, and third order neighbors for a pacing location marked with a star near the center of this view of the 490-lead sock mesh.

used the MHC or AME first guesses as the starting points for training data set refinement.

For the refinement of the training data set we tested three schemes whose schematic descriptions are illustrated in Fig. 3. The first refinement scheme used the correlation values from the first step to select the 12 most highly correlated maps as the training data set, which we referred to as "high-CC." The second and third schemes used the results of the first guess methods (MHC or AME maps) as their inputs. The second refinement method consisted of selecting the maps that had their earliest activation site within a 15 mm radius of the earliest activation site of the first-guess map. This scheme included the nearest spatial neighbors and we referred to it as "spatial activation." For these first two schemes, we experimented with different numbers of highly correlated beats for high-CC, and radius values for the spatial activation method, and found 12 maps and 15 mm, respectively, to perform the best.

The third scheme consisted of computing the range of activation times by subtracting the earliest activation value from the latest activation value within the first-guess map and identifying the region on the epicardium that included the first 25% of the activation range, known as the "early activated region" or EAR. The associated training data set then consisted of all the maps from the database that were stimulated from a site within this EAR, which we referred to as "temporal activation." When the number of maps in the temporal activation training set was greater than 50 we halved the percentage value that defined the EAR, and when the number of maps was less than 6, we doubled the percentage value.

We computed results using all these methods but will present in detail only those from the "MHC-Spatial activation" method, which started with the most highly correlated (MHC) map as the first guess and refined the training set according to spatial activation refinement method, and the "AME-Temporal activation" method, which used all-maps-estimate (AME) as the first guess and refined the training set with the temporal activation refinement scheme.

F. Presentation of Results

We present sample images and summaries of estimation errors for left and right ventricularly paced maps separately. To

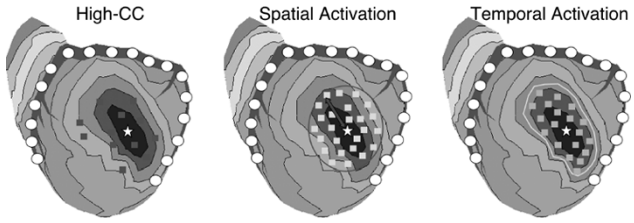

Fig. 3. Schematic descriptions of three different training set refinement schemes. Stars show the earliest site of activation of the first guess maps. Rectangles are the pacing sites for the maps selected with the refinement schemes called the high-CC, spatial activation, and temporal activation, from left to right. Refer to the text for the descriptions of each scheme.

most clearly reveal the earliest site of activation and the details of the activation sequence, we used local scaling for each of the activation maps, i.e., the mapping of value to color is specific to each case. In all maps, blue and red indicate early and late activation, respectively, and the spacing between isocontours was approximately 10 ms throughout. We included the earliest and the latest activation time values to the right bottom of each map as Min and Max values, respectively. Red tubes in the figures represent the coronary veins we used to select the surrogate catheter leads.

III. Results

A. Effect of Training Set Selection

Table I contains the results of comparing estimated maps created from the all-maps-estimate to those from the matched training sets using the LMap testing paradigm for left ventricular (LV) and right ventricular (RV) pacing separately. The table shows the trend of consistent improvement in estimation accuracy with the degree of matching between the test beat pacing site and those of the members of the training set. The improvement is more prominent for the maps with RV-pacing sites than LV-pacing sites. In only 6% of cases did the more closely matched training sets fail to bring about an improvement in localizing the earliest site of activation. In almost 74% of the maps, the first order neighbors set performed as well or better than training sets based on $\mathrm{F}+\mathrm{S}$ and $\mathrm{F}+\mathrm{S}+\mathrm{T}$. These results imply that some best-case accuracy was lost going to F from $\mathrm{F}+\mathrm{S}$ but that overall accuracy was improved in the tradeoff. Differences between the results based on different training sets were statistically significant for all error metrics. We also note that there was no difference in estimation performance between the maps coming from isolated hearts and those from the *in situ* preparation.

Fig. 4 contains examples of original and estimated activation maps for two specific cases—one from pacing the LV and one from the RV—using matched training sets. In both cases, the topographies of the maps support the statistical summary results. Estimates obtained from the first order neighbors most faithfully replicated the original high-resolution map. We note that the activation times were between 0 and 120 ms both in the originals and the estimates. We also note that all estimates perform credibly, both in terms of identifying the earliest site of activation and the entire structure of the activation sequence, especially given that they came from only 42 measurement sites distributed

TABLE I

SUMMARY OF ESTIMATION ERROR STATISTICS FOR DIFFERENT ORDERS OF NEIGHBORS IN THE TRAINING SETS FOR LEFT AND RIGHT VENTRICULARLY PACED MAPS USING THE LMAP TESTING PARADIGM. LDIST IS THE EUCLIDEAN DISTANCE BETWEEN THE EARLIEST ACTIVATION SITE OF THE ESTIMATED AND ORIGINAL MAPS. ΔT_{EA} IS THE ABSOLUTE DIFFERENCE OF THE EARLIEST ACTIVATION VALUES BETWEEN THE ORIGINAL AND THE ESTIMATED MAPS. VALUES ARE EXPRESSED AS MEANS $\pm$ STANDARD DEVIATIONS FOR LDIST AND ΔT_{EA}. ALSO INCLUDED ARE THE PERCENTAGES OF CASES WITH AN ERROR THAT WAS SMALLER THAN THE AVAILABLE RESOLUTION, I.E., THE DISTANCE BETWEEN ELECTRODES, (< MINRES), LDIST LESS THAN 5 mm (<5 mm), AND LDIST LESS THAN 10 mm (<10 mm). "ALL MAPS" INDICATES THAT ALL THE MAPS IN THE DATABASE EXCEPT FOR THE MAP TO BE RECONSTRUCTED (A TOTAL OF 469 ACTIVATION MAPS) WERE INCLUDED IN THE TRAINING SET. THE DIFFERENT ORDERS OF NEIGHBORS ARE DESCRIBED IN THE TEXT AND IN FIG. 2

Statistics for maps with LV-pacing sites					
Training Set	LDist	ΔT_{EA}	$< MinRes$ %	$< 5\ mm$ %	$< 10\ mm$%
All Maps	8.72 $\pm$ 6.39	16.44 $\pm$12.30	19	28	59
F+S+T	5.29 $\pm$ 4.40	11.03 $\pm$ 8.08	32	41	85
F+S	4.68 $\pm$ 3.76	8.53 $\pm$ 5.99	31	46	89
F	4.27 $\pm$ 3.20	6.13 $\pm$ 5.44	28	47	97
Maps with RV-pacing sites					
Training Set	LDist	ΔT_{EA}	$< MinRes$ %	$< 5\ mm$ %	$< 10\ mm$ %
All Maps	13.30 $\pm$ 7.78	22.85 $\pm$10.99	3	17	38
F+S+T	5.72 $\pm$ 3.22	14.92 $\pm$ 6.62	12	49	92
F+S	5.02 $\pm$ 3.11	9.54 $\pm$ 5.26	16	59	96
F	4.49 $\pm$ 2.43	5.94 $\pm$ 6.12	12	75	97

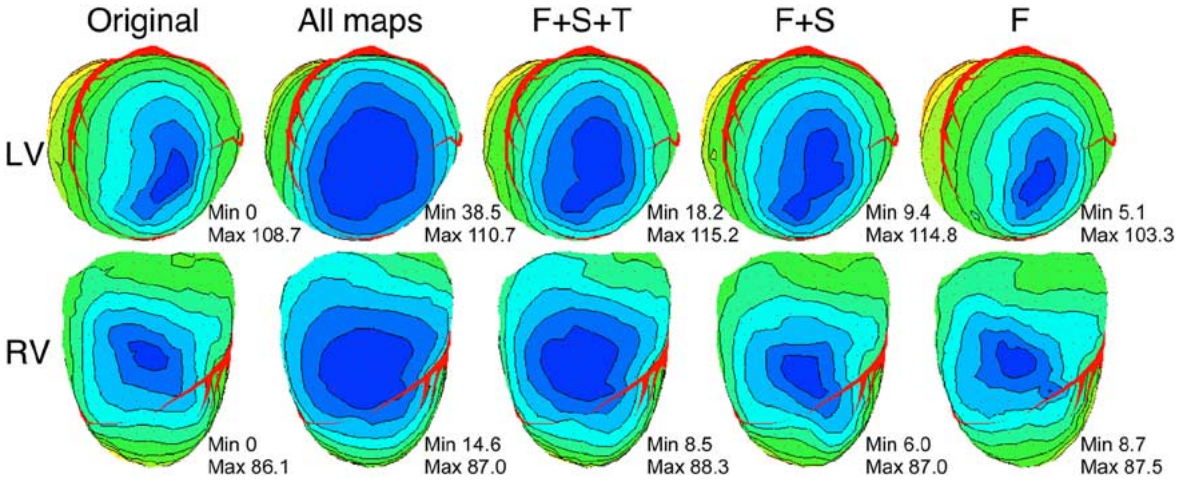

Fig. 4. Two examples of estimated activation maps using training sets composed of different orders of neighbors. This figure shows the original (left most column) and estimated activation maps for a map paced from the left ventricle (upper row) and right ventricle (lower row). The results from different training sets are included as marked in the figure. In order to highlight the activation pattern and the earliest site of activation, we used a different (local) scaling for each map. Blue and red indicate early and late activation, respectively. Activation values were between 0 and 120 ms both in originals and the estimates. There were offsets (ΔT_{EA}) in the earliest activation times but not significant differences in the latest activation values.

along the coronary veins. In both cases shown, the measurement sites were well separated (>20 mm) from the activation site.

B. Uninformed Selection of Training Sets

The first step in finding the best training set in the case of a test beat of unknown pacing site was to perform correlation analysis between test and candidate training beats based on the measured values from the 42 venous sites. This analysis revealed that in 67% of the test cases, the training map with the highest correlation was paced from a point within the first order neighborhood of the test map's pacing site. An additional 21% of cases came from the second order neighborhood and 7% came from the third order neighbors so that, in total, 95% of the test maps could be located within the first, second, or third order neighborhoods based only on a comparison of the 42 leads selected as surrogate venous catheter leads. The other approach for finding a good first estimate was the all-maps-estimate which showed that in 99% of the cases, the original site of the earliest activation was within the 25% early-activated region of the estimated map.

These findings from the first estimates set the stage for selecting the training data sets based on the three algorithms described above. Table II summarizes the results of estimating all the test maps with pacing sites on the LV and RV using the LMap testing paradigm. All refinement methods performed similarly and better than the all-maps-estimate; they also achieved results approximately as good as, and in some cases even better than, those from the second order neighbors training sets, a method that requires knowledge of the actual pacing site. The average correlation coefficient between the original and the estimated maps was very high (0.97) for all methods, indicating that these methods captured well the general pattern of epicardial activation. There was an average delay of approximately 10 ms between the earliest activation value in the estimated maps and the original test maps. Overall, estimation was more accurate for maps with LV pacing sites than RV pacing sites.

Fig. 5 shows two typical estimation results in which pacing sites were on the midanterior LV (upper row) and posterior RV (lower row). This figure demonstrates that all selection methods were more successful in determining an early-activated region

TABLE II

SUMMARY OF ESTIMATION ERROR STATISTICS FOR DIFFERENT METHODS OF REFINEMENT OF TRAINING SETS IN THE CASE OF LEFT AND RIGHT VENTRICULARLY PACED MAPS USING THE LMAP TESTING PARADIGM. IN THE HIGH-CC METHOD, THE 12 MOST HIGHLY CORRELATED MAPS WERE INCLUDED IN THE TRAINING SET. MHC-SPATIAL ACTIVATION METHOD STARTED WITH THE MOST HIGHLY CORRELATED MAP (MHC) AND REFINED THE TRAINING SET ACCORDING TO SPATIAL ACTIVATION REFINEMENT. AME-TEMPORAL ACTIVATION METHOD USED THE ALL-MAPS-ESTIMATE (AME) AND REFINED THE TRAINING SET WITH THE TEMPORAL ACTIVATION REFINEMENT SCHEME. THE FIRST LINE FOR BOTH LV AND RV CASES IS THE SAME AS PREVIOUS TABLE

Statistics for maps with LV-pacing sites					
Selection Method	LDist	ΔT_{EA}	$< MinRes$ %	< 5 mm %	< 10 mm %
All Maps	8.72 ± 6.39	16.44 ±12.30	19	28	59
High-CC	4.67 ± 4.02	8.65 ± 7.31	33	45	89
MHC-Spatial Activation	5.51 ± 4.11	10.42 ± 8.33	25	41	86
AME-Temporal Activation	4.98 ± 4.27	9.38 ± 7.22	32	45	86
Maps with RV-pacing sites					
Selection Method	LDist	ΔT_{EA}	$< MinRes$ %	< 5 mm %	< 10 mm%
All Maps	13.30 ± 7.78	22.85 ±10.99	3	17	38
High-CC	7.12 ± 6.58	11.96 ± 6.80	13	50	80
MHC-Spatial Activation	7.15 ± 5.85	10.63 ± 5.69	13	42	80
AME-Temporal Activation	7.80 ± 5.66	13.23 ± 6.81	10	43	74

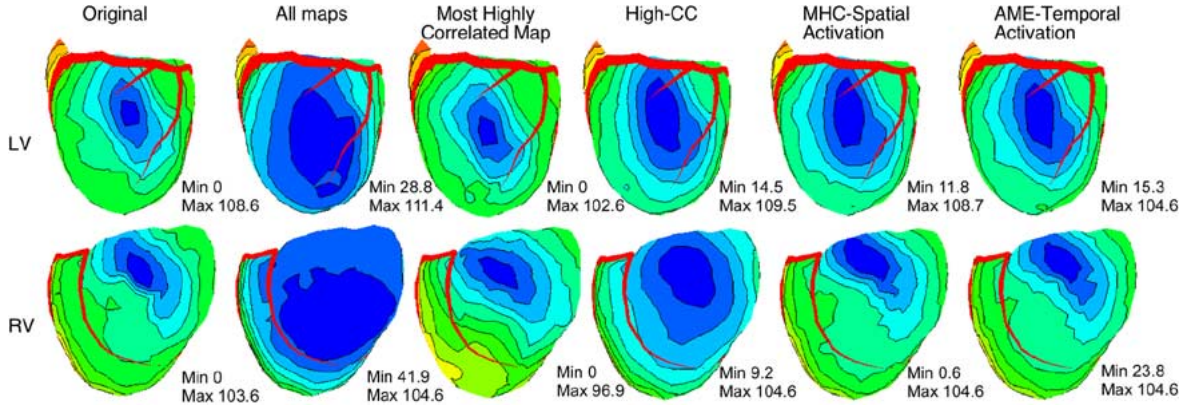

Fig. 5. Comparison between the original and the estimates using LMap testing paradigm from three methods for the maps with pacing sites on the LV (top row) and RV (bottom row). The leftmost column contains the original activation sequence. The second and third columns contain the all-maps-estimate first guess and the most highly correlated map, respectively. The fourth, fifth, and sixth columns contain results from training the covariance matrix with maps selected using the high-CC, MHC-Spatial, and AME-Temporal activation methods, respectively.

and the earliest site of activation than the all-maps estimate. The refinement methods produced similar results which all showed slightly broader early activated regions than the originals due to the smoothing effect of the estimation approach.

For the test maps that did not have pacing sites close to the surrogate measurement leads, the all-maps estimate tended to produce overly broad regions of early activation, leading to errors in localizing the site of activation, and therefore, errors in the training data set selection for the AME-Temporal activation method, which depends sensitively on the accuracy of the estimate of early activation. The all-maps estimate produced results comparable to those based on refined training sets only in cases in which the pacing site of the test map lay close to the surrogate catheter leads; even then, the error was a shift toward the closest catheter lead. Training sets based on the most highly correlated maps also incurred errors. When the training maps selected on the basis of neighborhood had activation sites that were relatively dispersed rather than tightly grouped, the resulting estimation sometimes showed dual sites of earliest activation.

IV. DISCUSSION

The aim of this study was to develop strategies for selecting training data sets for estimation of epicardial activation-time maps from venous catheter measurements. The driving hypothesis was that training data sets matched in some way to the test map would perform better than training sets containing a broader, more diverse, mix of maps. To test such a hypothesis, the challenge then became first identifying the criteria by which to perform the matching and then developing signal processing strategies by which to select those members of the training set that match a particular test case, given that the test data are, by definition, incomplete.

The choice of stimulation—or early activation—site as a matching criterion is quite natural for several reasons. The site at which the heart first activates has profound influence on the spread of excitation despite the role of the specialized conduction system. This influence is perhaps strongest for beats initiated from the epicardium because of the 20–50 ms required for activation to cross the ventricular wall, reach the conduction system, and then conduct in antegrade fashion to other parts of the heart [1]. Thus, it was likely that the site of earliest epicardial activation would provide a robust feature by which to organize and select members of a training data set. The first set of results in this report support this intuition by showing that selecting a training data set that includes beats with nearby pacing sites does, indeed, improve estimation accuracy. There was a consistent improvement in estimation accuracy with increased degree of matching of the training set. We obtained at least 4 mm improvement in the LDist and 10 ms in the ΔT_{EA} when we trained the transformation matrix

with maps paced from the first order neighbors, compared to all maps in the database.

With the general validity of the approach confirmed, the larger challenge then became one of establishing a means of selecting the appropriate beats for the training data set in the absence of knowledge of the true earliest site of activation. We tested two different first-guess approaches and three different training set refinement methods that used the first-guess results as their inputs. All approaches performed well on the maps with both LV and RV pacing sites, as measured using the LMap testing paradigms. We did note that performance was worst with pacing sites on the apex and RV freewall for all the methods we investigated. These and additional results not included here suggest that reduced performance might arise because of the low catheter accessibility to these regions and hence may be improved if more veins in the RV or close to the apex were accessible with the multi-electrode catheters.

Our study has focused entirely on beats paced from the epicardium, even though the bulk of clinical catheter mapping concentrates on the endocardium (see Darbar *et al.* [9] for a comprehensive recent review). The motivation for this choice was that for a substantial percentage of patients with postmyocardial infarction and nonischemic sustained ventricular tachycardias, critical pathways of reentry exist in the subepicardium so that ablation strategies directed only at the endocardium do not provide successful resolution of arrhythmias [34], [38], [39]. In addition, there now exist the required devices and technical experience to routinely probe the coronary veins with up to 20 electrodes on a single catheter. Clinicians already make use of the information from these catheters to reveal local electrical activity but are unable to identify and localize events that occur more than a few millimeters from the veins. Once there is adequate evidence to suggest epicardial involvement, there are also methods by which to bring radio-frequency ablation catheters to the critical sites and carry out treatment. Therefore, there exists both a need to develop techniques for mapping epicardial arrhythmias and an emerging diagnostic technology that could lead to a treatment paradigm. We note also that the techniques we have developed would almost certainly work equally well when applied to the endocardial surface as an activation mapping tool, perhaps enabling more rapid mapping of unstable dynamic rhythms from fewer catheter measurements. We concentrated in this study on epicardial mapping because lack of access is so much more severe that alternative mapping methods are unavailable even with unlimited time.

A critical question to address in a study like this is what level of the spatial resolution is required for clinical utility. One source of an answer is the size of lesions from radio frequency (RF) catheters, which lie in the range of 7–8 mm in diameter and 8–9 mm in depth from a standard 8-mm RF catheter [10]. Additional factors include the fact that most cases involve a sequence of lesions (7 ± 5 [21] and 12 ± 10 [8] according to the literature), each following slight movement of the catheter in order to ensure adequate coverage. Finally, other approaches, for example those using electrocardiographic inverse solutions [27], [29], have reported maximal accuracy in the range of 8–10 mm. In light of these facts, the target accuracy of our refinement methods of 10 mm for 85% of the cases seem reasonable.

Limitation of this study include that the database did not include data from hearts with large regions of conduction block or in which we observed reentry. Preliminary (unpublished) results from a small number of test beats with large areas of previous myocardial infarction suggest that while localizing the earliest site of activation may be feasible, there will be difficulties in predicting the entire activation sequence when the infarcted regions lie far from the venous catheters. Ongoing experiments will provide the data to develop training sets that include such profoundly altered hearts.

Moreover, in this study some of the beats in the database came from the same animal as the test beat. The practical reason for this is clear but nonetheless this might cause results to be overly optimistic, and in addition might cause some other biases. Ongoing experiments will provide a separate test set from the training set which will include different animals, different pacing sites, and different disease conditions.

One possible weakness in the study is that the high-resolution mapping data for the database needs to be acquired during open chest procedures, and our catheter-based estimation method requires a closed chest approach. Green *et al.* [16] have described the effect of conductivity of the volume conductor on activation time and potentials. In that study, they showed clearly that activation sequence does not depend on the volume conductor, even to the point that taking the heart completely out of the volume conductor. We also note that one reason for our choice of activation time as the parameter to be estimated is its robustness.

Although we have shown that an estimation-based approach to epicardial mapping is quite feasible and accurate, its application to clinical practice will require overcoming additional technical hurdles. Perhaps the first is the need to acquire high-resolution epicardial maps with which to build the necessary database. Obtaining such data does require direct access to the heart. However, open-chest surgery is still a relatively frequent occurrence for such procedures as valve repair and replacement and coronary artery bypass grafts. The time required during such procedures to obtain epicardial maps is just minutes, so that it should not present substantial additional burden to the patient.

An additional challenge to applying this technique in a clinical setting will be determining the relationship between venous catheter locations and the corresponding sites in the high-density epicardial sock array. For this, we anticipate using fluoroscopic images obtained during the catheterization procedure. A study into the impact of estimation error in localizing electrode locations is currently underway in our laboratory.

Catheter leadset selection is another important aspect of the estimation technique that ongoing studies are designed to address. The topics of these studies will include the effects of the number of leads to be selected and their relative locations on the coronary veins on reconstruction accuracy, and the sensitivity of the estimation approach to different types of simulated errors on the catheter leads.

Although the approach we present does not solve a formal inverse problem, it does provide results that are essentially identical to those of electrocardiographic inverse solutions, i.e., an activation map on the epicardial surfaces. In some recent examples, Oster *et al.* [29] and Modre *et al.* [27] have both reported reconstruction of single pacing sites to within 8–10 mm, comparable with at least some of our results. However, the cost of creating an inverse solution is substantially larger than our approach. An inverse solution requires the creation of a patient-specific geometric model, typically based on results from

a tomographic imaging study using CT or MRI, followed by a computationally costly procedure. Our approach, by contrast, requires no geometric information other than the location of the catheters relative to a normalized epicardial potential electrode array. Computation of the estimation of the activation sequence is also quite straightforward. The most relevant observation may be that these two approaches are complementary rather than competing. An estimate of activation may well serve as a constraint of an otherwise standard inverse solution, an approach we are currently pursuing [35].

The results of this study encourage further investigation and provide adequate evidence that an epicardial mapping approach based on intravenous catheter measurements is feasible and can provide adequate accuracy for clinical applications. Furthermore, the approaches we propose for training data set selection can be easily automated so that consistent optimization is possible. With the advances in transthoracic access to the pericardial space in order to apply catheter ablation of cardiac arrhythmias [7], [34], [36], [39], [41], such an estimation approach will complement this type of treatment as a minimally invasive diagnosis technique.

ACKNOWLEDGMENT

The authors gratefully acknowledge J. Davis, M. Allison, Dr. P. Ershler, and B. Steadman at the CVRTI, for their assistance in the experiments. They also thank Dr. J. Stinstra at the CVRTI for his thoughtful suggestions.

REFERENCES

[1] G. Arisi, E. Macchi, C. Corradi, R. L. Lux, and B. Taccardi, "Epicardial excitation during ventricular pacing: relative independence of breakthrough sites from excitation sequence in canine right ventricle," *Circ. Res.*, vol. 71, no. 4, pp. 840–849, 1992.

[2] G. E. Beatty, S. C. Remole, M. K. Johnston, J. E. Holte, and D. G. Benditt, "Non-contact electrical extrapolation technique to reconstruct endocardial potentials," *PACE*, vol. 17, no. 4, p. 765, 1994.

[3] S. V. Beiden, M. A. Maloof, and R. F. Wagner, "A general model for finite-sample effects in training and testing of competing classifiers," *IEEE Trans. Pattern Anal. Machine Intell.*, vol. 25, no. 12, pp. 1561–1569, Dec. 2003.

[4] A. Berruezo, L. Mont, S. Nava, E. Chueca, E. Bartholomay, and J. Brugada, "Electrocardiographic recognition of the epicardial origin of ventricular tachycardias," *Circ.*, vol. 109, pp. 1842–1847, 2004.

[5] T. R. Betts, P. R. Roberts, S. A. Allen, and J. M. Morgan, "Radiofrequency ablation of idiopathic left ventricular tachycardia at the site of earliest activation as determined by noncontact mapping," *J. Cardiovasc. Electrophysiol.*, vol. 11, pp. 1094–1101, 2000.

[6] J. C. Bezdek, L. O. Hall, and L. P. Clarke, "Review of MR image segmentation techniques using pattern recognition," *MedPhys*, vol. 20, pp. 1033–1048, 1993.

[7] J. Brugada, A. Berruezo, A. Cuesta, and J. Osca, "Nonsurgical transthoracic epicardial radiofrequency ablation A alternative in incessant ventricular tachycardia," *J. Amer. Coll. Cardiol.*, vol. 41, pp. 2036–2043, 2003.

[8] H. Calkins, "Cooled ablation," *J. Cardiovasc. Electrophysiol.*, vol. 15, pp. S12–S17, Oct. 2004.

[9] D. Darbar, J. E. Olgin, J. M. Miller, and P. Friedman, "Localization of the origin of arrhythmias for ablation: from electrocardiography to advanced endocardial mapping systems," *J. Cardiovasc. Electrophysiol.*, vol. 12, no. 10, pp. 1309–1325, 2001.

[10] A. d'Avila, C. Houghtaling, P. Gutierrez, O. Vragovic, J. N. Ruskin, M. E. Josephson, and V. Y. Reddy, "Catheter ablation of ventricular epicardial tissue A comparison of standard and cooled-tip radiofrequency energy," *Circ.*, vol. 109, pp. 2363–2369, 2004.

[11] J. M. T. de Bakker, M. J. Janse, J. J. L. van Capelle, and D. Durrer, "Epicardial mapping by simultaneous recording of epicardial electrograms during cardiac surgery for ventricular aneurism," *J. Amer. Coll. Cardiol.*, vol. 2, pp. 947–953, 1983.

[12] N. M. S. de Groot, M. Bootsma, E. T. van der Velde, and M. J. Schalij, "Three-dimensional catheter positioning during radiofrequency ablation in patients: first application of a real-time position management system," *J. Cardiovasc. Electrophysiol.*, vol. 11, pp. 1183–1192, 2000.

[13] M. Eldar, D. G. Ohad, J. J. Goldberger, Z. Rotstein, S. Hsu, D. K. Swanson, and A. J. Greenspon, "Transcutaneous multielectrode basket catheter for endocardial mapping and ablation of ventricular tachycardia in the pig," *Circ.*, vol. 96, pp. 2340–2437, 1997.

[14] M. N. Faddis, W. Blume, J. Finney, A. Hall, J. Rauch, J. Sel, K. T. Bae, M. Talcott, and B. Lindsay, "Novel magnetically guided catheter for endocardial mapping and radiofrequency catheter ablation," *Circ.*, vol. 106, pp. 2980–2985, 2002.

[15] L. Gepstein and S. J. Evans, "Electroanatomical mapping of the heart: Basic concepts and implications for the treatment of cardiac arrhythmias," *PACE*, vol. 21, no. 6, pp. 1268–1278, 1998.

[16] L. S. Green, B. Taccardi, P. R. Ershler, and R. L. Lux, "Epicardial potential mapping: effects of conducting media on isopotential and isochrone distributions," *Circ.*, vol. 84, pp. 2513–2521, 1991.

[17] I. Guyon, J. Makhoul, R. Schwartz, and V. Vapnik, "What size test set gives good error rate estimates?," *IEEE Trans. Pattern Anal. Machine Intell.*, vol. 20, no. 1, pp. 52–64, Jan. 1998.

[18] M. J. Janse, "Reentrant arrhythmias," in *The Heart and Cardiovascular System*, 2nd ed, H. A. Fozzard, E. Haber, R. B. Jeenings, A. M. Katz, and H. E. Morgan, Eds. New York: Raven, 1992, vol. II, ch. 79, pp. 2055–2094.

[19] H. M. Kalayeh and D. A. Landgrebe, "Predicting the required number of training samples," *IEEE Trans. Pattern Anal. Machine Intell.*, vol. 5, no. 6, pp. 664–666, Nov. 1983.

[20] W. Kaltenbrunner, R. Cardinal, M. Dubuc, M. Shenasa, R. Nadeau, G. Tremblay, M. Vermeulen, P. Savard, and P. L. Page, "Epicardial and endocardial mapping of ventricular tachyarrhythmia in patients with myocardial infarction. Is the origin of the tachycardia always subendocardially localized?," *Circ.*, vol. 84, pp. 1058–1071, 1991.

[21] H. Kottkamp, G. Hindricks, X. Chen, J. Brunn, S. Willems, W. Haverkamp, M. Block, G. Breithardt, and M. Borggrefe, "Radiofrequency catheter ablation of sustained ventricular tachycardia in idiopathic dilated cardiomyopathy," *Circ.*, vol. 92, pp. 1159–1168, 1995.

[22] R. O. Kuenzler, "Generating Epicardial Activation Order From Multielectrode Venous Catheters," M.S. thesis, Univ. Utah, Salt Lake City, 1998.

[23] R. O. Kuenzler, R. S. MacLeod, B. Taccardi, Q. Ni, and R. L. Lux, "Estimation of epicardial activation maps from intravascular recordings," *J. Electrocardiol.*, vol. 32, no. 2, pp. 77–92, Apr. 1999.

[24] L. Littmann, R. H. Svenson, J. J. Gallagher, J. G. Selle, S. H. Zimmern, J. M. Fedor, and P. G. Colavita, "Functional role of the epicardium in postinfarction ventricular tachycardia," *Circ.*, vol. 83, pp. 1577–1591, 1991.

[25] R. L. Lux, M. Akhtar, and R. S. MacLeod, "Mapping and invasive analysis," in *Foundations of Cardiac Arrhythmias: Basic Concepts and Clinical Approaches*, P. M. Spooner and M. R. Rosen, Eds. New York: Marcel Dekker, 2001, ch. 15, pp. 393–424.

[26] R. S. MacLeod and C. R. Johnson, "Map3d: Interactive scientific visualization for bioengineering data," in *Proc. IEEE Engineering in Medicine and Biology Soc. 15th Annu. Int. Conf.*, 1993, pp. 30–31.

[27] R. Modre, B. Tilg, G. Fischer, and P. Wach, "Noninvasive myocardial activation time imaging: a novel inverse algorithm applied to clinical ECG mapping data," *IEEE Trans Biomed. Eng.*, vol. 49, no. 10, pp. 1153–1161, Oct. 2002.

[28] Q. Ni, R. S. MacLeod, R. L. Lux, and B. Taccardi, "A novel interpolation method for electric potential fields in the heart during excitation," *Annal. Biomed. Eng.*, vol. 26, no. 4, pp. 597–607, 1998.

[29] H. S. Oster, B. Taccardi, R. L. Lux, P. R. Ershler, and Y. Rudy, "Noninvasive electrocardiographic imaging: Reconstruction of epicardial potentials, electrograms, and isochrones and localization of single and multiple electrocardiac events," *Circ.*, vol. 96, no. 3, pp. 1012–1024, 1997.

[30] W. H. Press, B. P. Flannery, S. A. Teukolsky, and W. T. Vetterling, *Numerical Recipes: The Art of Scientific Computing*. New York: Cambridge Univ. Press, 1986.

[31] J. S. Sanchez, R. Barandela, A. I. Marques, R. Alejo, and J. Badenas, "Analysis of new techniques to obtain quality training sets," *Pattern Recogn. Lett.*, vol. 24, no. 7, pp. 1015–1022, Apr. 2003.

[32] M. J. Schalij, F. P. van Rugge, M. Siezenga, and E. T. van der Velde, "Endocardial activation mapping ventricular tachycardia in patients: First application of a 32-site bipolar mapping electrode catheter," *Circ.*, vol. 98, pp. 2168–2179, 1998.
[33] R. J. Schilling, N. S. Peters, and D. W. Davies, "Simultaneous endocardial mapping in the human left ventricle using a noncontact catheter: Comparison of contact and reconstructed electrograms during sinus rhythm," *Circ.*, vol. 9, pp. 887–898, 1998.
[34] R. A. Schweikert, W. I. Saliba, G. Tomassoni, N. F. Marrouche, C. R. Cole, T. J. Dresing, P. J. Chou, D. Bash, S. Beheiry, C. Lam, L. Kanagaratnam, and A. Natale, "Percutaneous pericardial instrumentation for endo-epicardial mapping of previously failed ablations," *Circ.*, vol. 108, pp. 1329–1335, 2003.
[35] Y. Serinagaoglu, D. H. Brooks, and R. S. MacLeod, "Bayesian solutions and performance analysis in bioelectric inverse problems," *IEEE Trans. Biomed. Eng*, vol. 52, no. 6, pp. 1009–1020, Jun. 2005.
[36] E. Sosa, M. Scanavacca, A. D'Avila, F. Oliviera, and J. A. F. Ramires, "Nonsurgical transthoracic epicardial ablation to treat recurrent of ventricular tachycardia," *J. Amer. Coll. Cardiol.*, vol. 35, no. 1, pp. 1442–1449, 2000.
[37] E. Sosa, M. Scanavacca, A. D'avila, J. Piccioni, O. Sanchez, J. L. Velarde, M. Silva, and B. Reolao, "Endocardial and epicardial ablation guided by nonsurgical transthoracic epicardial mapping to treat recurrent of ventricular tachycardia," *J. Cardiovasc. Electrophysiol.*, vol. 9, pp. 229–239, 1998.
[38] E. Sosa, M. Scanavacca, A. D'avila, and F. Pilleggi, "A new technique to perform epicardial mapping in the electrophysiology laboratory," *J. Cardiovasc. Electrophysiol.*, vol. 7, pp. 531–536, 1996.
[39] V. Swarup, J. B. Morton, M. Arruda, and D. J. Wilber, "Ablation of epicardial macroreentrant ventricular tachycardia associated with idiopathic nonischemic dilated cardiomyopathy by a percutaneous transthoracic approach," *J. Cardiovasc. Electrophysiol.*, vol. 12, no. 10, pp. 1164–1168, 2002.
[40] S. Tadjudin and D. A. Landgrebe, "Covariance estimation with limited training samples," *IEEE Trans. Geosci. Remote Sensing*, vol. 37, no. 4, pp. 2113–2118, Jul. 1999.
[41] C. Vahlhaus, H. J. Bruns, J. Stypmann, T. D. Tjan, F. Janssen, M. Schafers, H. H. Scheld, O. Schober, G. Breithardt, and T. Wichter, "Direct epicardial mapping predicts the recovery of left ventricular dysfunction in chronic ischaemic myocardium," *Eur. Heart J.*, vol. 25, no. 2, pp. 151–157, Jan. 2004.
[42] F. H. M. Wittkampf, E. F. D. Wever, R. Derksen, A. A. M. Wilde, H. Ramanna, R. N. W. Hauer, and E. R. de Medina, "Localiza: New technique for real-time 3-dimensional localization of regular intracardiac electrodes," *Circ.*, vol. 99, pp. 1312–1317, 1999.
[43] B. Yilmaz, R. S. MacLeod, S. Shome, B. B. Punkse, and B. Taccardi, "Minimally invasive epicardial activation mapping from multielectrode catheters," in *Proc. IEEE Engineering in Medicine and Biology Soc. 23th Annu. Int. Conf.*, 2001.

Bülent Yılmaz received the B.S. degree in 1997 and the M.S. degree in 1999 in electrical and electronics engineering from Middle East Technical University, Ankara, Turkey, in 1997 and 1999, respectively. He received the Ph.D. degree from the University of Utah, Salt Lake City, in 2004.

He is currently an Assistant Professor in the Biomedical Engineering Department, Başkent University, Ankara, Turkey. His research interests are in biomedical signal and image processing. Specific current interests include forward and inverse problems in electrocardiography and electroencephalography.

Robert S. MacLeod (S'87–M'87) received the B.S. degree in engineering physics in 1979 and the Ph.D. degree in physiology and biophysics in 1990 from Dalhousie University, Halifax, N.S., Canada. He received the M.S. degree in electrical engineering from the Technische Universitat, Graz, Austria, in 1985.

He is an Associate Professor in the Bioengineering Department and the Department of Internal Medicine (Division of Cardiology) at the University of Utah, Salt Lake City, and an Associate Director of the Scientific Computing and Imaging Institute and the Nora Eccles Harrison Cardiovascular Research and Training Institute. His research interests include computational electrocardiography (forward and inverse problems), experimental investigation and clinical detection of cardiac ischemia and repolarization abnormalities, and scientific computing and visualization.

Bonnie Billard Punske received the B.S. and M.S. degrees in mechanical engineering from the University of Arizona, Tucson, in 1986 and 1989, respectively. She received the Ph.D. degree in biomedical engineering in 1997 from the University of North Carolina at Chapel Hill.

She is an Assistant Professor in the Department of Internal Medicine, Division of Cardiology and the Department of Bioengineering, University of Utah, Salt Lake City, and a Faculty Member of the Nora Eccles Harrison Cardiovascular Research and Training Institute. Her research interests include electrical and optical imaging and graphic visualization of the spread of excitation, sequence of repolarization, and arrhythmias in normal and genetically altered hearts.

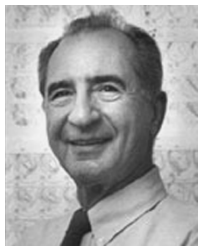

Bruno Taccardi received the M.D. degree in 1946 from State University of Milan, Milan, Italy, and the Ph.D. degrees in 1951 and 1961 in physiology from the University of Brussels, Brussels, Belgium, and the University of Pavia, Pavia, Italy, respectively.

He is currently a Research Professor in the Department of Internal Medicine, University of Utah, Salt Lake City, and the Associate Director of the Nora Eccles Harrison Cardiovascular Research and Training Institute. His research interests include biophysics of cardiac electric fields, three-dimensional mapping of potential and current distributions associated with excitation and recovery, and genesis of the electrocardiogram, experimental study, and computer simulation.

Dana H. Brooks (S'87–M'91) received the B.A. degree in english in 1972 from Temple University, Philadelphia, PA, and the B.S.E.E., M.S.E.E., and Ph.D. degrees in electrical engineering from Northeastern University, Evanston, IL, in 1986, 1988, and 1991, respectively.

He is an Associate Professor of electrical and computer engineering, Associate Director of the Center for Communications and Digital Signal Processing, a member of the Institute for Complex Software Systems and the Center for Subsurface Sensing and Imaging Systems, and PI of the BioMedical Imaging and Signal Processing Laboratory, all at Northeastern University, and a member of the Center for Bioelectric Field Modeling, Simulation, and Visualization headquartered at the University of Utah, Salt Lake City. He was a Visiting Professor during 1999–2000 at the Universitat Politecnica de Catalunya, Barcelona, Spain. His research interests lie in application of statistical and digital signal and image processing to biomedical signal processing and medical and biological imaging, and in open-source software systems for these applications.